Analysis of Combustion Characteristics in Diesel Flame by Means of Chemiluminescence

H.Fujimoto, H.Iida, T.Aoyama* and J.Senda

Department of Mechanical Engineering
Doshisha University
1-3 Tatara Miyakodani, Tanabe-cho, Tsuzuki-gun, Kyoto 610-03
Japan
* *Toyota Motor Co.*

ABSTRACT

A diesel flame shows the complex process with the chemical reaction. Nevertheless, there are few papers dealing with the measurement of chemical species, such as OH radical. The paper presented here makes clear the spatial and temporal distribution of this OH radical in a diesel flame in a piston cavity of a bottom view diesel engine by use of interference filters not by that of an expensive excimer laser. Also, the same distributions of flame temperature and KL factor are shown in the paper, by applying the two-color method. From these experimental results, the authors find the strong relation among emission intensity of OH radical, flame temperature and KL factor.

INTRODUCTION

It is very difficult to detect chemical species in a diesel flame, because the strong emission intensity of a luminous soot in it is very strong. However, the species must be measured with some method, in order to clarify the complex diesel combustion processes. The authors showed already the detecting system of OH and CH radicals in a diesel flame which was developing in a bottom view small sized high-speed DI diesel engine by use of photonic multi-channel analyzer in the previous papers[1),(2)]. However, the emission intensities of these species were very weak and were measured at a given time as cumulative data over many cycles. Generally speaking, combustion processes in a diesel engine are the non-steady phenomena and fluctuate not only in every cycle but also at the same spatial point. Then, the temporal and spatial data must be detected to understand the diesel combustion phenomena.

In the experiments presented here, the temporal data of OH radical at a given measuring point was measured in the optical engine mentioned above by means of the optical fiber-interference filter system in order to get the temporal data, under this standpoint. The radical appears in the region of the combustion reaction where the oxygen exists[3)] and has the close relation to the thermal NO in the enlarged Zeldvich mechanism[4)]. The data were treated, considering the probability density, because the phenomena were statistical. Also the flame temperature and KL factor in the same diesel flame were measured through the same optical path, applying the two-color method[5)]. Then, these three data were compared with each other, and the relation among them were discussed in order to clarify the diesel combustion phenomena.

LUMINESCENT PROCESS OF OH RADICAL

In a flame of hydrocarbons[3)], C_2 radical is generated at the initial stage of the thermal pyrolysis of hydrocarbon itself. Then, CH radical is formed by the following reaction:

$$C_2 + OH = CH^* + CO \qquad (1)$$

where * expresses the excited state. Succeeding this process, OH radical is produced by the reaction as follows:

$$CH + O_2 = CO + OH^* \qquad (2)$$

In both reactions, there is enough exothermic reaction to excite chemical species. Then, the luminescence of band spectrum appears, when the transition of chemical species from the excited state to the lower energy level is proceeding. The intensity of this luminescence is depending on the product of the concentration of the excited chemical species and the probability of its transition to the ground state, and is not directly proportional to the concentration itself.

OH radical appears mainly in the combustion region where the oxygen exists, because its concentration corresponds to those of CH radical and oxygen owing to eq. (2)[3)]. However, the luminescence of OH radical occurs in some degree independent on the combustion reaction, as the excited OH radical is produced at the equilibrium state of the reversible reaction in the reaction zone with a high temperature of the flame[2)]. CH radical takes part in the formation of prompt NO and OH radical is related to that of thermal NO in the enlarged Zeldvich mechanism.

ELIMINATION OF BACKGROUND LIGHT DUE TO LUMINOUS SOOT

The continuous radiant spectrum due to the luminous soot must overlap the emission wavelength of the objective OH radical which lies at the region of near ultraviolet radiation.

Then, it is surely necessary for detection of the luminescence of OH radical to eliminate this spectrum. In the experiments, three interference filters were used for the detection and the elimination as shown in Fig.1. The filters F1, F2 and F3 had the center transmitted wavelength of 293.5nm, 307.7nm and 318.7nm, and their half band width were 3.5nm, 5.9nm and 3.9nm, respectively. Emission intensity of luminous soot at the sides of short and long wavelengths were obtained by F1 and F2. Then, the intensity of the background light of the luminous soot was detected by the linear approximation between outputs of F1 and F2. F3 shows the emission intensity of OH radical with that of the luminous soot. So, the emission intensity of OH radical itself was detected by the subtraction of the former intensity with the approximate intensity from the latter one. Then, the temporal information on the emission intensity was got at a given measuring point.

USED ENGINE WITH OPTICAL SYSTEM

Fig.2 shows the used engine of a water-cooled 4 stroke DI diesel engine with a single cylinder. The diameter of cylinder and the stroke were 92mm and 96mm, respectively. The effective compression ratio was 19.3. A piston①equipped with a quarts window ② was connected with an elongated piston③. The diameter of cavity was 50mm and its depth was 15mm. The volume of this cavity was as same as that of the base engine. The top clearance at the squish area was 0.18mm. The engine was motored in advance by a dynamometer at a revolutional speed of about 600 r.p.m.. During this duration the fuel oil was injected out of the engine through a sub-nozzle④. Once the engine satisfied the given condition, the fuel oil was injected into the combustion chamber through a main nozzle⑤ operated by a solenoid valve⑥. The number of nozzle hole was 4, its diameters of nozzle hole was 0.26mm and the opening pressure of nozzle was 21.0MPa. The revolutional speed at the firing was about 1000r.p.m.. The load was none due to the restriction of the optical system. The injection quantity was 22.0mg/*l* cycle, the excess air ratio was 2.2 and the swirl ratio was 2.0. The used fuel oil was JIS second class gas oil. The coolant temperature was 353K constant.

The light from the flame was passing through the quarts window and was reflected by a mirror⑦. The reflected light was converged through a condenser lens⑧whose focal length was 200mm at the end surface of an optical fiber⑨branching off the light in 4 equalizing energy. Every 3 branched lights reached the interference fibers⑩ of F1, F2 and F3, respectively. Thereafter, their intensities were transformed into voltage through photomultipliers⑪ . The light of a He-Ne laser incidented through a one branch of the optical fiber in order to adjust the optical axis. Each signal of 40 cycles at each measuring region was recorded on the wavememory⑫at every sampling clock of 0.5 deg.CA, that is, 83 μ s, eliminating the first two cycles. However, the history of transmissivity was different at each measuring region because of the adhesion soot on the window. Then, the data were not sampled, when the transmissivity showed under 70%. I n the preliminary experiments, the sampling clock was set 2 μ s in order to examine the accuracy.

Fig.3 displays the measuring points in the combustion chamber. The focus of condenser lens was set on the bottom of the piston at the top dead center. The region , that is, the measuring space was the combination of the same two truncated cones whose diameter of the top was 3mm at the focal surface and the vertical angle was as same as the solid angle of the condenser lens. Namely, the emission of radical measured as the mean value of the optical length in this measuring space. 49 points located in every 4mm at the half part of the combustion chamber.

The flame temperature and the KL factor were measured by two-color method . Two interference filters of 502nm and 652nm in the center transmitted wavelength were equipped instead of those for the OH radical measurement shown in Fig.2. Their half band width were 9nm and 12nm, respectively. The flame temperature and the KL factor were calculated by use of the ensemble mean values of every outputs for the continuous 15 cycles at each measuring points, eliminating first two cycles after firing.

Fig.4 shows the cylinder pressure, its standard deviation,

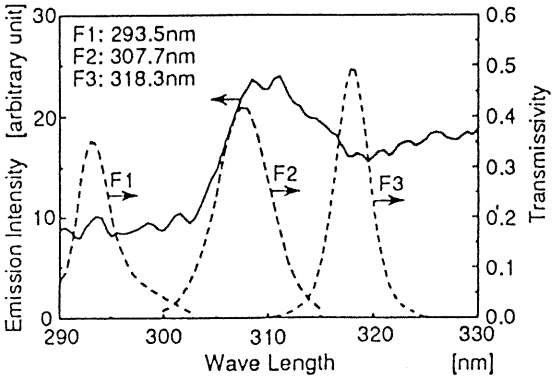

Fig.1 Band spectrum of OH radical and transmissivity of used interference filters

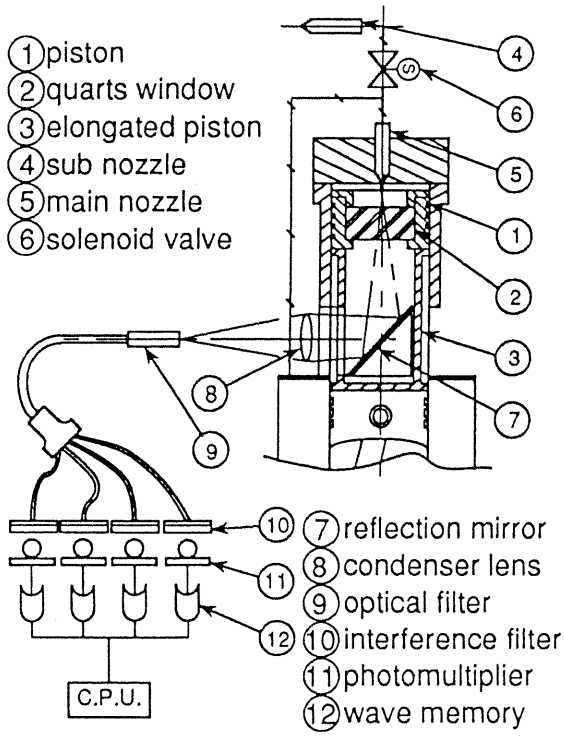

Fig.2 Used engine with optical system

the heat release rate, the nozzle needle lift and the injection pressure, averaged from 3rd to 13th cycle after the firing. The ignition delay is about 8.0 deg. CA and the maximum cylinder pressure is 7.3MPa. The rapid rise in the heat release rate appears after the ignition and it reaches the maximum of 105J/deg.CA at 2.0deg.CA BTDC. The heat release finishes at about 17.0deg.CA ATDC.

CYCLE VARIATION IN EMISSION INTENSITY OF OH RADICAL

Fig.5 is one of examples of histories of the cylinder pressure and the outputs of three interference filters for arbitrary continuous five cycles. The wavelength of E(307.7nm) is corresponding to the emission of OH radical. There is large cycle variation in each quantity. Fig.6 shows three typical histograms of the emission intensity of OH radical at a given crank angle against time series data for continuous sampled 40 cycles. The histogram is like a Gaussian distribution in case (a), it shows a wider distribution in case (b) and there is many peeks in case (c). Then, the maximum in the first case, the median in the second case and the peak when there appears more frequency around it than around the other peak were taken as the representative value. However, (b) and (c) are rare cases.

The data must be treated statistically in discussion because of the trend such as Fig.6. The first usual treatment is the standard deviation. However, the data of the emission intensity include not only its fluctuation but also the probability of its existence, although the scale of measuring space is relatively smaller than the ununiformity of combustion field in the experiments. Namely, the standard deviation becomes larger inevitably at the timing when and at the space where the relatively higher intensity appears. Therefore, the second treatment is the relative standard deviation defined as the quotient of the standard deviation to the mean value of the intensities. It reveals the grade of the fluctuation against the mean value.

The probability of the existence of flame in the measuring space must be considered as well as the emission intensity of OH radical, because the number of flame is 4 and the flame is moving with the swirl motion. Then, peak values at a given crank angle of the flame temperature and the KL factor derived from histograms like Fig.6 for continuous sampled 15 cycle are decided as the representative one. And only the standard deviation is calculated as the statistical treatment.

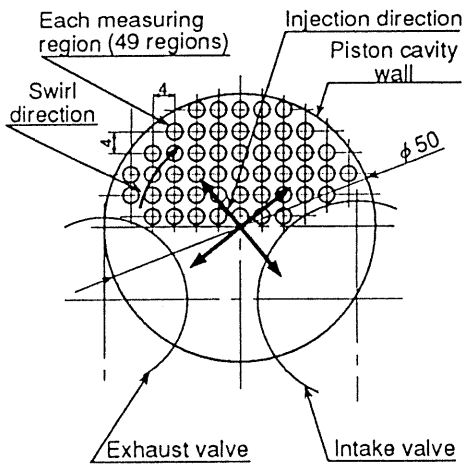

Fig.3 Measuring regions of flame in combustion chamber

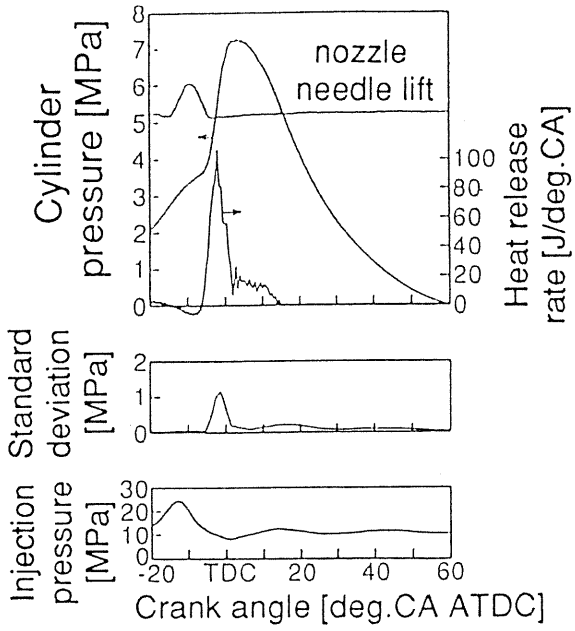

Fig.4 General performance of used engine

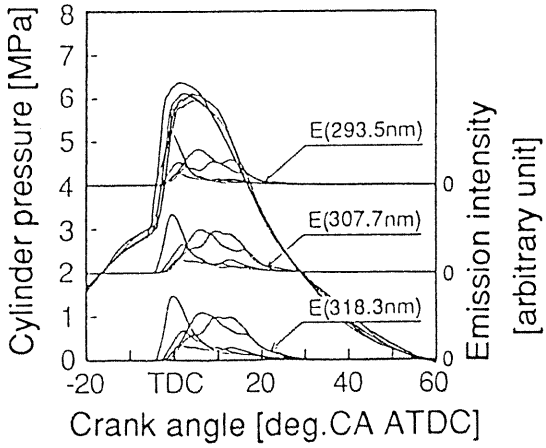

Fig.5 Example of histories of cylinder pressure and outputs of three interference filters

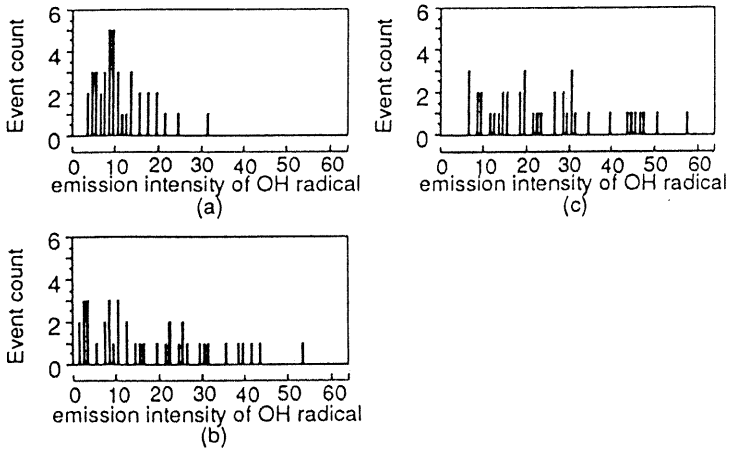

Fig.6 Typical histograms of emission intensity of OH radical

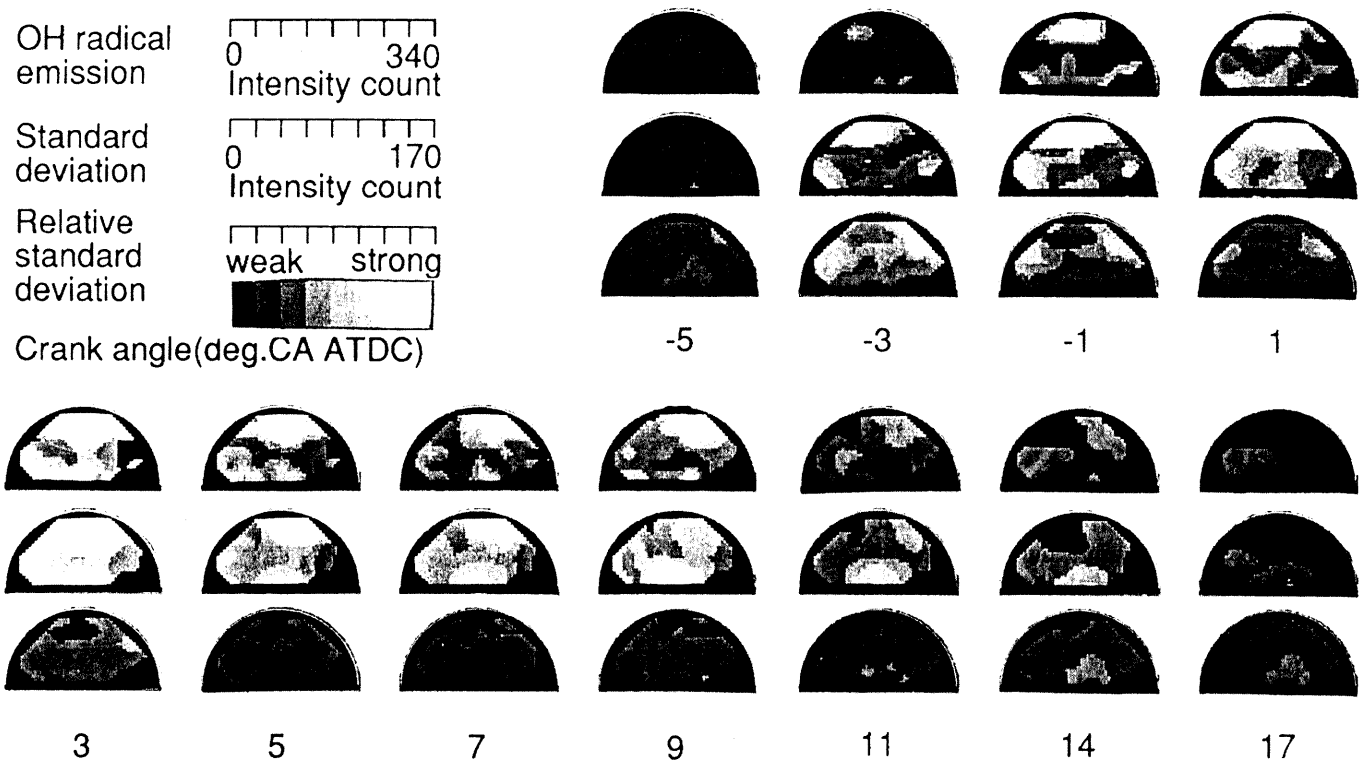

Fig.7 Spatial and temporal distributions of emission intensity of OH radical, their standard deviations and their relative standard deviations

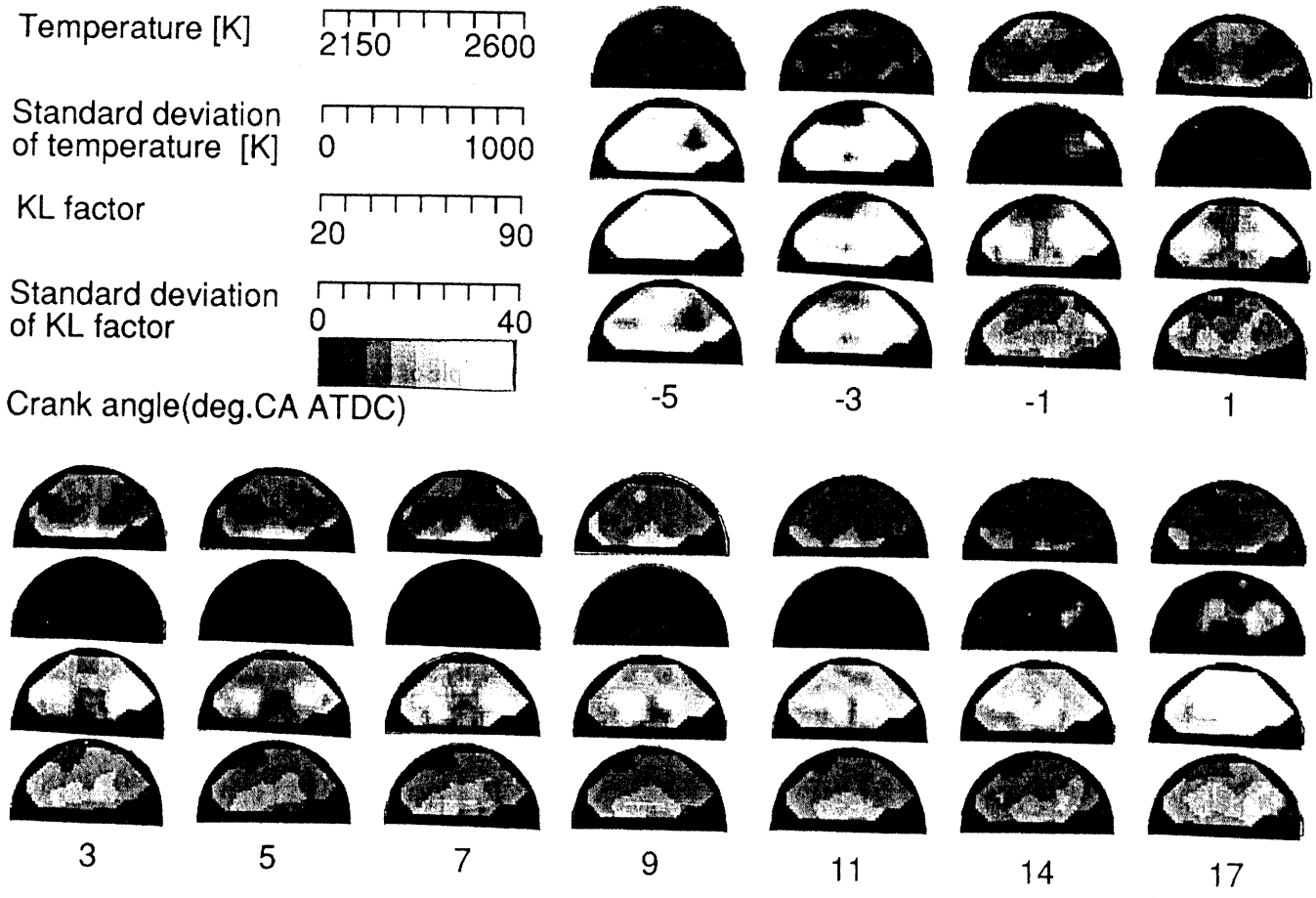

Fig.8 Spatial and temporal distributions of flame temperature , KL factor and their standard deviations

the mean value of the intensities. It reveals the grade of the fluctuation against the mean value.

The probability of the existence of flame in the measuring space must be considered as well as the emission intensity of OH radical, because the number of flame is 4 and the flame is moving with the swirl motion. Then, peak values at a given crank angle of the flame temperature and the KL factor derived from histograms like Fig.6 for continues sampled 15 cycle are decided as the representative one. And only the standard deviation is calculated as the statistical treatment.

DISTRIBUTION OF EMISSION INTENSITY OF OH RADICAL

Fig.7 shows the spatial and temporal distributions of emission intensity of OH radical, its standard deviation and its relative standard deviation with 8 gradation. Scarcely appears OH radical until 5.0 deg.CA BTDC, although the ignition breaks out at 8.0 deg.CA BTDC on the curve of the heat release rate, because the burning like a pre-mixed flame controls the combustion process, the spatial ununiformity of burning is remarkable, then, the local rate of burning reaction is low during this duration. At 3.0 deg.CA BTDC, the emission of OH radical is observed at the region of the downstream side of the swirl keeping a little off the direction of injection and the diffusion burning is starting from this region. After 1.0 deg.CA BTDC, the region of the strong emission intensity is moving in the downstream direction of the swirl motion from the region mentioned above. The reasons of this tendency are : (1) the quantity of air existing in the spray increases by the effects of the impingement on the wall of piston cavity, (2) the air is stagnant more in the downstream region than in the upstream region and (3) the quantity of combustible mixture is formed more and the burning reaction is more active in the downstream region. At 3.0 deg.CA ATDC, the strong intensity appears near the nozzle outlet. This is the reason why the initial part of spray where the equivalence ratio is very high is collapsed by the stop of the momentum supply to the spray after the injection, then, the lump of large droplets is falling down with drift near the nozzle outlet and then the diffusion burning is progressing. Therefore, the emission intensity is weakening gradually until the end of combustion.

Generally speaking, the standard deviation is large in the region of the high emission intensity of OH radical. In the distribution of the relative standard deviation, it is large during the period from 5.0 to 1.0 deg.CA BTDC as the evidence of the large fluctuation of the burning. After 1.0 deg.CA BTDC, it becomes smaller.

DISTRIBUTIONS OF FLAME TEMPERATURE AND KL FACTOR

Fig.8 is the spatial and temporal distributions of the flame temperature, the KL factor and their standard deviations. At 7.0 deg.CA BTDC, there are no flame temperature and KL factor because the luminous flame does not appear. From 5.0 to 3.0 deg.CA BTDC, the standard deviations of both flame temperature and KL factor are very high during this duration because the burning like a pre-mixed flame in which the quantity of soot is very smaller than that in the diffusion burning is predominant. Then, both quantities can not be detection. During the period from 1.0 deg.CA BTDC to 5.0 deg.CA ATDC, the high flame temperature appears in the downstream side of the swirl motion near the wall of piston cavity. The region is corresponding to that of the high emission intensity of OH radical. After 7.0 deg.CA ATDC, the region of high temperature lies only near the nozzle exit due to the burning of the lump of large droplets. At 1.0 deg.CA BTDC, the region of the high standard deviation of the flame temperature appears at the leading edge of impinging part of the spray, as the burning starts at this region. Thereafter, the small standard deviation is shown near the nozzle outlet. Again the medium standard deviation appears in the medium region of the combustion chamber owing to the ununiformity of the evaporated fuel.

The distribution of KL factor shows generally the reverse tendency of those of flame temperature and emission intensity of OH radical. The high KL factor appears mainly near the spray axis where the droplets density is high. The large standard deviation of the KL factor distributes in wider region than that of the flame temperature. The standard deviation is large at the region of the upstream side of the swirl keeping a little off the spray axis. After 7.0 deg.CA ATDC, the high standard deviation exists in the region near the nozzle exist as same as the flame temperature. Therefore, the medium standard deviation is confirmed in the medium region of the combustion chamber as well as that of the flame temperature.

AVERAGE VALUES OF FLAME TEMPERATURE, KL FACTOR, EMISSION INTENSITY OF OH RADICAL AND HEAT RELEASE RATE AGAINST CRANK ANGLE

Fig.9 displays the flame temperature, the KL factor and the emission intensity of OH radical averaged for the measured

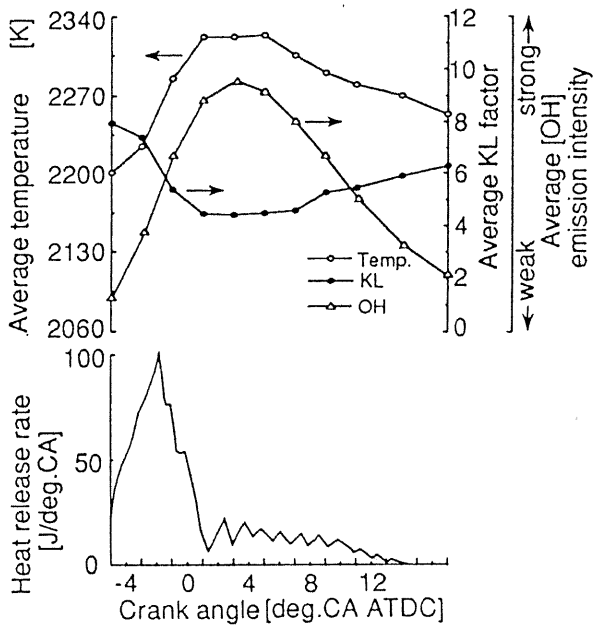

Fig.9 Averaged values of flame temperature, KL factor, emission intensity of OH radical and heat release rate against crank angle

data of the all measuring points with progress of crank angle. The heat release rate is also shown in the figure. The average temperature which is related to the mean temperature calculated by the gas law gets its maximum later than heat release rate. The tendency has presented in many previous experiments. The history of the flame temperature has very close relation to that of the emission intensity of OH radical. It is notable that the timing of the strongest emission intensity corresponds to that of the highest flame temperature. Namely, OH radical is obviously connected with the burning reaction also the generation of the thermal NO. The tendency of the KL factor shows the reverse history of the flame temperature also as presented in many previous papers.

CORRELATION AMONG EMISSION INTENSITY OF OH RADICAL, FLAME TEMPERATURE AND KL FACTOR

Fig.10 shows the correlation between the emission intensity of OH radical and the flame temperature, Fig.11

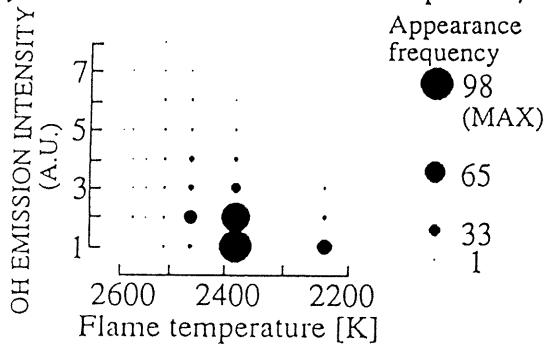

Fig.10 Correlation between emission intensity of OH radical and flame temperature

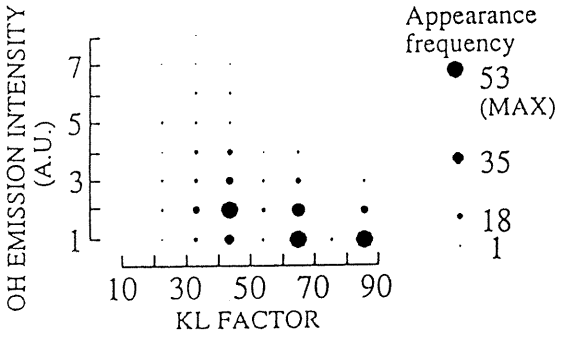

Fig.11 Correlation between emission intensity of OH radical and KL factor

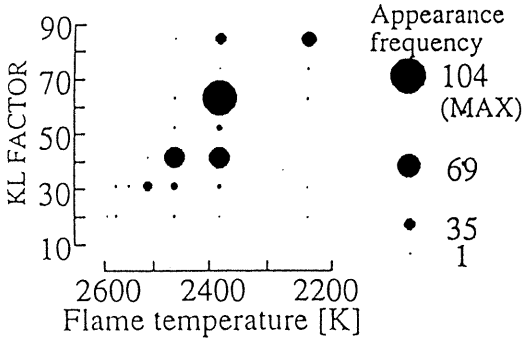

Fig.12 Correlation between KL factor and flame temperature

expresses that between the former quantity and the KL factor and Fig.12 displays that between the KL factor and the flame temperature, with 8 gradation from 1.0 deg.CA BTDC to 17.0 deg.CA ATDC when the diffusion burning is predominant. The size of the black circle is proportional to their appearance frequency. The higher the flame temperature is, the stronger the emission intensity of OH radical is. The emission is relatively weak, when the flame temperature is low. This correlation is the marked matter, although the scatter is pretty large. The tendency of the correlation between the emission intensity of OH radical and the KL factor shown in Fig.11 is completely contrary to that displayed in Fig.10. The KL factor becomes smaller, as the flame temperature becomes higher,as shown in Fig.12. The scattering is the smallest in these correlations. As a consequence, the region of the strong emission intensity of OH radical is limited to that of the high flame temperature, and the soot generates in the region of the low flame temperature.

CONCLUSIONS

The following conclusions are drawn from the experiments:
(1) The emission intensity of OH radical is very weak and its relative standard deviation is very large during the period of the burning like a pre-mixed flame.
(2) In the period of diffusion burning, the emission intensity of OH radical is large in the region of the vigorous combustion, and its relative standard deviation is small.
(3) The region of the strong emission intensity of OH radical is limited to that of the high flame temperature.
(4) Comparing with averaged values for the whole region of measuring points, the timing of the strongest emission intensity of OH radical corresponds to that of the highest flame temperature, and the history of the former has the close correlation with that of the latter.
(5) The higher the flame temperature is, the lower the KL factor is.

REFERENCES

(1) Kimura, N., Aoyama, T., Hamamura, Y., Senda, J., and Fujimoto,H.,"Flame Characteristics in D.I.Diesel Engine with a Transparent Piston", Trans.JSAE, Vol.23, No2, pp.9-14,1992.(in Japanese)
(2)Aoyama,T.,Hokuto,H.,Kotoh,F.,Senda,J.,and Fujimoto,H.,"Combustion Characteristics by use of Chemiluminescence in Diesel Flame ,"Trans. JSAE, Vol.24,No.4,pp.53-57,1993.(in Japanese)
(3) Mizutani,Y., Combustion Engineering, Morikita Shuppan, Tokyo, pp.194-198,1989.(in Japanese)
(4) Tsujishita,M.,Iponmatsu,M.,and Hirano,A., "The Dependence of NO,CH and OH Distribution on the Equivalence Ratio in CH4/Air Flames Using a Planar Laser Induced Fluorescence", Nensho Kenkyu, No.94,pp33-43,1993.(in Japanese)
(5) Matsui,Y.,Kamimoto,T.,Matsuoka,S.,and Oguri,A.,"A Study on the Measurement of Flame Temperature in Diesel Engine ,"Trans. JSME,Vol.44,No.377,pp.228-238,1978.(in Japanese)